ISSN 1063-7834, Physics of the Solid State, 2019, Vol. 61, No. 2, pp. 192–200. © Pleiades Publishing, Ltd., 2019.
Russian Text © E.V. Bogdanov, E.I. Pogoreltsev, M.V. Gorev, M.S. Molokeev, I.N. Flerov, 2019, published in Fizika Tverdogo Tela, 2019, Vol. 61, No. 2, pp. 330–338.

LATTICE DYNAMICS

Effect of Deuteration on Phase Transitions in Vanadium Dioxotetrafluoride

E. V. Bogdanov[a, b, *], E. I. Pogoreltsev[a, c], M. V. Gorev[a, c], M. S. Molokeev[a, c], and I. N. Flerov[a, c]

[a] *Kirensky Institute of Physics, Siberian Branch, Russian Academy of Sciences, Krasnoyarsk, 660036 Russia*

[b] *Institute of Engineering Systems and Energetics, Krasnoyarsk State Agrarian University, Krasnoyarsk, 660049 Russia*

[c] *Institute of Engineering Physics and Radioelectronics, Siberian Federal University, Krasnoyarsk, 660074 Russia*

**e-mail: evbogdanov@iph.krasn.ru*

Received August 13, 2018

Abstract—The crystals of $(ND_4)_3VO_2F_4$ with a high degree of deuteration (~87%) have been grown and a significant (~1.5%) increase in the unit cell volume has been detected. The decrease in the chemical pressure leads to a change in the sequence of phase transitions due to wedging-out of one of the rhombic phases observed in $(NH_4)_3VO_2F_4$. The thermal physical studies have been carried out and the entropies, deformations, and pressure coefficients related to structural transformations have been determined. The *T*–*p* phase diagram has been built and the pressure and temperature boundaries of crystal phase stability have been determined. The dielectric studies demonstrate a nonferroelectric nature of the phase transitions in $(ND_4)_3VO_2F_4$. The experimental and model entropies are compared. Based on the decrease in the entropy as a result of deuteration, a hypothesis on significant but not limited anharmonism of vibrations of ammonia tetrahedral corresponding to the disordering is proposed.

DOI: 10.1134/S1063783419020082

1. INTRODUCTION

To develop new polar materials, polar basis blocks are often used, since their presence in a structure can lead to the appearance of a macroscopic dipole moment. The application of asymmetric blocks such as polyhedrons of transition metals or individual cation pairs was advantageous when synthesizing new polar materials with a nonlinear-optical activity [1–5].

The crystal structure of complex oxyfluorides consists of $[MeO_xF_{6-x}]$ polar anions [6]. Oxyfluoride octahedra can form various configurations: linear $(CuNbOF_5(H_2O)(pyz)_3$ [7]), zigzag $(CuWO_2F_4(H_2O)(py)_2$ [8]) chains, or they have a spiral motive $(AMoO_2F_4(H_2O)_2(pyz)$ [9]). The spiral chains are, as a rule, ordered, the zigzag chains are disordered, and linear chains of $[MeO_xF_{6-x}]$ octahedra have either an orientation order or disorder. The disordering of oxyfluoride octahedra is caused by close sizes and the electronegativity of oxygen and fluorine anions. The methodology of designing ordered oxyfluoride materials is a preparation of isotropic media around oxyfluoride octahedrons that would lead to the ordering of oxygen and/or fluorine atoms. To do this, the optimization of the space of interoctahedral voids [10], the comparison of the polarizabilities [11] and/or the introduction of various cations [12] are usually used.

Vanadium oxyfluorides (VOF) can form various distorted oxyfluoride octahedra due to the capability of vanadium atoms to change their valence states [13]. The existence of two different binding motives around a central vanadium atom (V–O bond and V–F bond) forms high-symmetric local coordination spheres that can lead to a nonlinear optical behavior such as the generation of the second optical harmonic [14].

However, in spite of the variety of vanadium oxyfluorides (VOF), the oxyfluoride anion in most of them is disordered, and the completely ordered state was only observed in $K_2VO_2F_3$ crystals [15], the structure of which consists of chains connected by the VOF octahedrons angles. The ferroelectric and proton-conducting states were observed in vanadium oxyfluoride $(NH_4,K)_3VO_2F_4$ [16]. The compound belongs to a family of elpasolites and has the rhombic symmetry (space group *Immm*) at room temperature.

The symmetry of the $(NH_4)_3VO_2F_4$ crystal at room temperature was first defined as a rhombic with two equally probable space groups *Immm* and *I*222, but the preference was given to the first variant [17]. The

phase transitions in this oxyfluoride were studied in detail in [18, 19]. According to the data of optical studies, $(NH_4)_3VO_2F_4$ undergoes four subsequent phase transitions with the following changes in the symmetry: $Fm\bar{3}m \leftrightarrow Immm(I222) \leftrightarrow rhombic \leftrightarrow P112/m \leftrightarrow P\bar{1}$ [18]. The calorimetric studies confirmed the existence of the first-order phase transitions at temperatures: $T_1 = 438$ K, $T_2 = 244$ K, $T_3 = 210$ K, and $T_4 = 205$ K. An analysis of the transformation entropies enabled one to correct the model of orientational disordering of VOF anions in the cubic phase [17]. The inclusion of vanadium atom disordering during the refinement of the crystal structure of $(NH_4)_3VO_2F_4$ single crystal in X-ray diffraction studies made it possible to postulate to a high degree of probability space group $I222$ for the rhombic phase existing in the temperature range $T_1 > T > T_2$ [20]. It was assumed that ammonium tetrahedrons and oxyfluoride octahedra are disordered and partially disordered in the initial cubic $Fm\bar{3}m$ and the first distorted $I222$ phases, respectively. The formation of twins with different orientations at $T < T_2$ prevented the refinement of the structures of the second rhombic, monoclinic, and triclinic phases [17, 20].

The problem of the role of cation/anion polyhedrons in the mechanism of structural distortions during the phase transitions in complex fluorides and oxyfluorides was studied repeatedly [21–23]. The substantial role of ammonia cation in ordering/disordering of fluoroxygen structures with isolated $(NH_4)_2Me^{6+}O_2F_4$ (Me^{6+}: W, Mo) was established when studying the compounds synthesized by substituting of univalent cation for the ammonia group [24] and also by its deuterization [25, 26].

In this work, the studies of the influence of deuteration of ammonia cation on the processes of disordering/ordering that are observed in oxyfluorides with bound anion polyhedrons are performed for the first time for the vanadium dioxytetrafluoride (V)–$(ND_4)_3VO_2F_4$ crystal.

2. EXPERIMENTAL AND RESULTS

The crystallization of the initial $(NH_4)_3VO_2F_4$ compound was carried out by fluorination of ammonium vanadate with addition of ammonia at temperature $T \approx 150$–200°C [20]

$$NH_4VO_3 + 2 \cdot NH_4OH + 4 \cdot HF = (NH_4)_3VO_2F_4 + 3 \cdot H_2O.$$

The obtained $(NH_4)_3VO_2F_4$ crystals dissolved in heavy water (99.9% D). The solution was held in an desiccator with phosphorus pentaoxide P_2O_5 up to complete absorption of the water and the start of the compound crystallization. To increase the degree of substitution D → H, we performed repeated recrystallization. The degree of deuteration was controlled at each cycle by comparing the integral ^{1}H NMR absorption lines of proton and deuterated compounds. As a result, we obtained small (~1 mm^3) $(ND_4)_3VO_2F_4$ crystals of yellow color, with the degree of deuteration of ~87%.

The data on the $(ND_4)_3VO_2F_4$ structure at room temperature were obtained using a Bruker D8 ADVANCE (radiation CuK_α) powder diffractometer and VANTEC linear detector ($2\theta \approx 0.016°$, $t \approx 0.5s/2\theta$).

The refinement of the model of the structure by the Rietveld method (Fig. 1) was performed using the TOPAS 4.2 program [27]. The main peaks were indexed in the rhombic cell. It is impossible to prefer any of space groups *Immm* or *I*222. Table 1 gives the unit cells parameters for space group *Immm* that are closer to the parameters found for the initial $(NH_4)_3VO_2F_4$ crystal [17, 20]. The final refinement of the structure led to low values of the *R*-factors (Table 1).

To determine the influence of deuteration on the phase transition temperature and energy parameters, we studied the heat capacity of the $(ND_4)_3VO_2F_4$ crystals. At low temperatures $T \approx 95$–310 K, the measurements were carried out using the precise methods of adiabatic calorimetry. A sample with mass $m \approx 1.2$ g was hermetically packed into an indium capsule in an inert helium atmosphere. The calorimetric measurements were performed in mode of continuous ($dT/dt \approx 0.15$ K/min) and discrete ($\Delta T \approx 2.5$–3.0 K) heatings. The heat capacity of the furniture consisting of the heater and the indium capsule was measured in a special experiment.

The studies at high temperatures $T \approx 315$–460 K were carried out by the differential scanning calorimetry (NETZSCH 204 *F*1). The sample with mass $m \approx$

Table 1. Main parameters of the refinement of the structure of the $(ND_4)_3VO_2F_4$ crystal

Compound	$(ND_4)_3VO_2F_4$
Sp.Gr.	*Immm*
a, Å	9.1334 (6)
b, Å	18.833 (1)
c, Å	6.2701 (5)
V, Å^3	1078.5 (1)
Z	6
2θ-interval, deg	5–90
R_{wp}, %	16.10
R_p, %	12.44
R_{exp}, %	14.45
χ^2	1.11
R_B, %	3.83

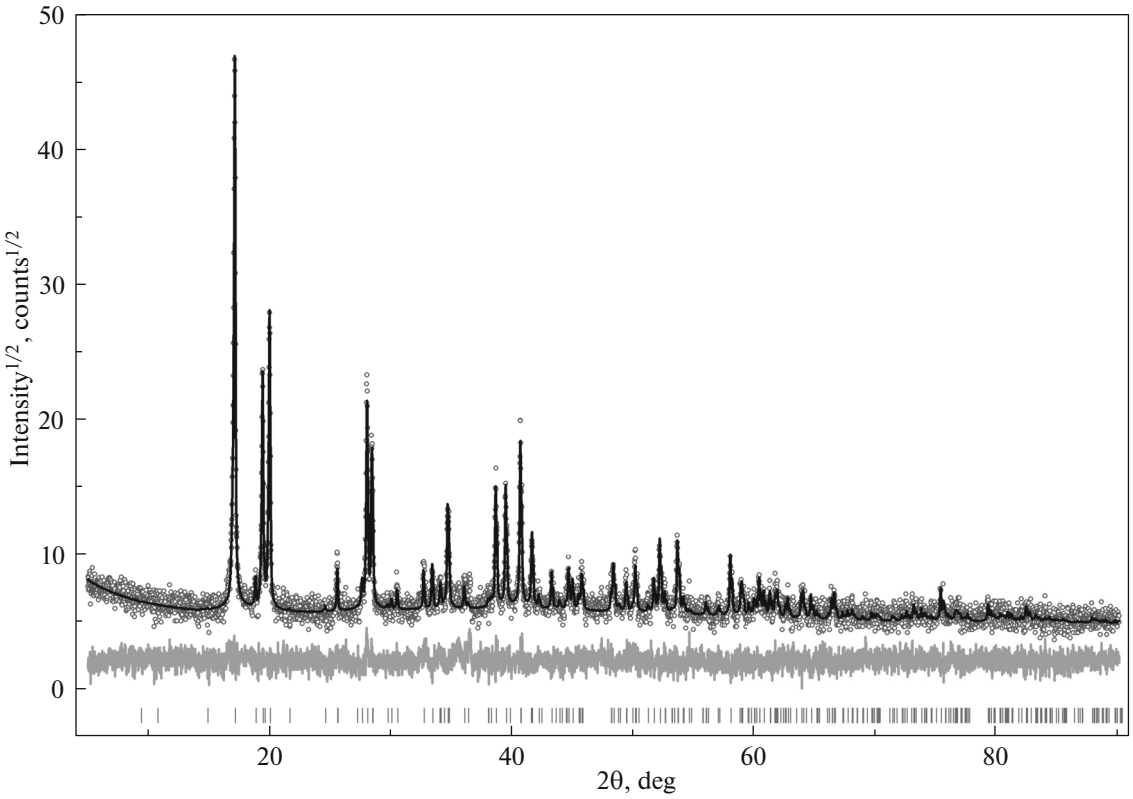

Fig. 1. Results of the refinement of the model of the $(ND_4)_3VO_2F_4$ structure by the Rietveld method.

0.025 g was placed in an aluminum container. The measurements were performed in a helium flow (20 mL/min) at a heating rate $dT/dt \approx 5$ K/min. A quartz standard was used to determine the absolute heat capacity of the sample.

The temperature dependence of the heat capacity of the $(ND_4)_3VO_2F_4$ crystal has three anomalies C_p (Fig. 2) at temperatures close to the phase transition temperatures T_1, T_3, and T_4 observed in the $(NH_4)_3VO_2F_4$ crystal (Table 2). Thus, the anomaly observed in proton compound near $T \approx 244$ K [19] was not observed in the deuterated crystal; i.e., this crystal does not undergo the *Immm*(*I*222) ↔ *rhombic* phase transition. Thus, for convenience of comparing the characteristics of the transitions, the low-temperature peaks of $C_p(T)$ of the $(ND_4)_3VO_2F_4$ crystal are denoted T_3 and T_4 (Table 2).

The anomalous increase in $C_p(T)$ observed at $T >$ 440 K is related to the start of the crystal decomposition process that is intensively developed at temperature $T' \approx 480$ K and is accompanied by the decrease in the sample mass. To obtain reliable data on the thermodynamic parameters of the phase transitions at T_1, the heat capacity was measured on several samples.

To determine the integral characteristics of the phase transitions, we divided total heat capacity C_p into regular lattice C_l and anomalous $\Delta C_p = C_p - C_l$ components. The experimental data on $C_p(T)$ far from the anomalous temperature ranges were interpolated by a polynomial dependence with the extrapolation to the phase transition regions (Fig. 2a).

The integration of the excess heat capacity $\Delta C_p(T)$ enabled us to obtain the information on the changes in

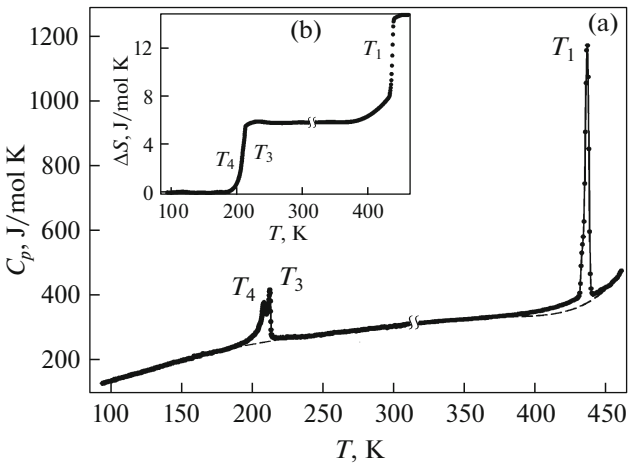

Fig. 2. Temperature dependences of (a) the heat capacity and (b) the phase transition entropy in the $(ND_4)_3VO_2F_4$ crystal over wide temperature range.

Table 2. Some thermodynamic parameters of the phase transitions in oxyfluorides $(ND_4)_3VO_2F_4$ and $(NH_4)_3VO_2F_4$ (T_C is the Curie temperature, N_i is the degree of proximity of the phase transition in the tricritical point)

Parameter	$(ND_4)_3VO_2F_4$	$(NH_4)_3VO_2F_4$ [19]
T_1, K	436.6 ± 0.5	438 ± 1
ΔS_1, J/mol K	8.7 ± 0.9	9.7 ± 1.0
$(dT_1/dp)_{calc}$, K GPa^{-1}	130	–
T_2, K	–	244.0 ± 0.2
ΔS_2, J/mol K	–	0.18 ± 0.04
T_3, K	212.10 ± 0.05	210.2 ± 0.2
$(A_T^2/B)_{T3}$, J/mol K^2	−0.8	−0.4
$(A_T^3/C)_{T3}$, J/mol K^3	5.8	1.1
$T_3 - T_{C3}$, K	2.2	1.4
N_3	−0.12	−0.1
ΔS_3, J/mol K	4.8 ± 0.6	6.2 ± 0.7
$(dT_3/dp)_{exp}$, K GPa^{-1}	−43 ± 5	−27 ± 3
$(dT_3/dp)_{calc}$, K GPa^{-1}	−40 ± 10	–
T_4, K	208.1 ± 0.1	205.1 ± 0.2
$(A_T^2/B)_{T4}$, J/mol K^2	−2.8	−1.3
$(A_T^3/C)_{T4}$, J^2/mol^2 K^3	2.8	2.2
$T_4 - T_{C4}$, K	0.1	0.4
N_4	−0.02	−0.05
ΔS_4, J/mol K	1.00 ± 0.12	0.80 ± 0.12
$(dT_4/dp)_{exp}$, K GPa^{-1}	−77 ± 5	−25 ± 3
$(dT_4/dp)_{calc}$, K GPa^{-1}	−70 ± 20	–

the enthalpy related to the high-temperature phase transition $\Delta H_1 = 3700 \pm 350$ J/mol and the sequence of low-temperature transformations $\Delta H_3 + \Delta H_4 = 1200 \pm 90$ J/mol. In the latter case, the determination of only the summary value $\Sigma\Delta H$ is due to the difficulties of separating individual enthalpy contributions, because of very close values T_3 and T_4.

The temperature behavior of the linear thermal expansion was studied in the temperature range $T \approx$ 120–485 K using a NETZSCH DIL402C dilatometer at a heating rate $dT/dt = 3$ K/min. The measurements were carried out in an inert helium atmosphere (the flow rate is of 50 mL/min). The thermal expansion of the measurement system was determined in a special experiment on the quartz standard sample. The samples for the dilatometric experiments were prepared as pellets ($d = 8$ mm, $h = 2$–3 mm) by pressing ($\Delta p \approx$ 2 GPa) without subsequent heat treatment because of the existence of ammonium cation in the study compound.

The temperature dependences of the volume deformation $\Delta V/V_0 = 3(\Delta L/L_0)$ (Fig. 3a) and the coefficient of volumetric thermal expansion $\beta = 3\alpha$ (Figs. 3b and 3c) demonstrate the anomalous behavior near the phase transition temperatures found in the calorimetric experiments. The anomaly character is found to be dependent on the thermal pre-history of the sample and the existence/absence of mechanical stresses in it. During the first heating of the sample in the initial stressed state appeared upon pressing the pellets, we observed significant stepwise deformation $\delta(\Delta V/V_0) \approx 2\%$ at temperature T_1 (Fig. 3a) and $\delta(\Delta V/V_0) \approx 0.5\%$ at temperatures near T_3 and T_4 (curve *1* in Fig. 3a). Upon heating to temperatures $T_1 < T < 450$ K, the sample is likely to be annealed as the results of repeated measurements show. The jump $\delta(\Delta V/V_0)$ significantly decreased at T_1 and the sign becomes negative for anomalies at T_3 and T_4: $(\delta V/V_0)_3 \approx -0.19\%$ and $(\delta V/V_0)_4 \approx -0.07\%$ (curve *2* in Fig. 3a).

As the $(ND_4)_3VO_2F_4$ crystal is heated to $T > 450$ K, we observe the anomalous behavior of $\beta(T)$ with a maximum at temperature $T' \approx 480$ K (Fig. 3b) at which the crystals decompose as was also observed in the calorimetric measurements.

The pressure sensitivity of the phase transition temperatures was studied by the method of differential thermal analysis (DTA). The hydrostatic pressure ($p \leq$ 0.5 GPa) was generated in a "piston–cylinder" vessel with a multiplicator, using silicon oil in the measurement chamber. The sample mass was $m \approx 0.025$ g. A copper-germanium thermocouple was used as a DTA thermoelement, and a quartz sample was used as a standard.

The specific features of the DTA setup design did not enable us to carry out the measurements in the region of the high-temperature phase transition. During the low-temperature studies at the atmospheric pressure, two anomalies were detected in the DTA signal at temperatures $T_3 = 212 \pm 1$ K and $T_4 = 209 \pm 1$ K (Fig. 4) that is a good agreement with the data of the calorimetric and dilatometric measurements (Table 2). An increase in pressure leads to a decrease in the phase transition temperatures with significantly different negative pressure coefficients.

The dielectric properties were measured in the temperature range $T \approx$ 100–300 K using an E7-20 immittance meter ($\nu = 1$ kHz) in mode of heating and cooling ($dT/dt = 0.7$ K/min). The leaf gold electrodes were deposited on the samples for measuring $\varepsilon(T)$ prepared as pressed ($\Delta p \approx 2$ GPa) pellets ($d = 8$ mm, $h =$ 0.7–1 mm) that were not subjected to heat treatment.

The temperature dependence of the dielectric permittivity demonstrate anomalous behavior near the phase transitions at T_3 and T_4 related to small changes in the permittivity $\Delta\varepsilon_3 = 1.7$ and $\Delta\varepsilon_4 = 1.2$ (Fig. 5a).

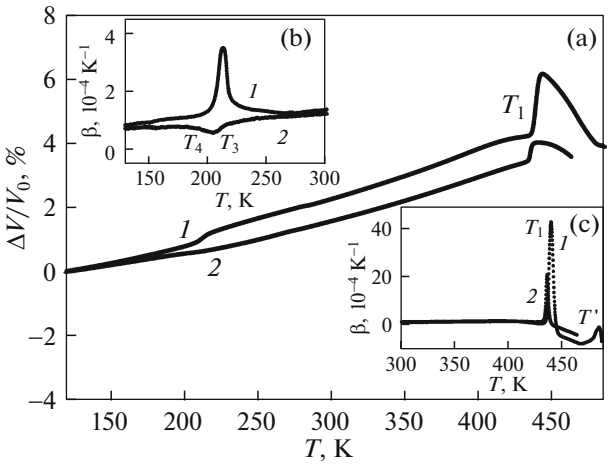

Fig. 3. Temperature dependences (a) of the spontaneous deformation of the $(ND_4)_3VO_2F_4$ crystal (*1*) in the initial stressed state and (*2*) after annealing at $T > T_1$ and the coefficient of volume expansion in the (b) low-temperature and (c) high-temperature regions.

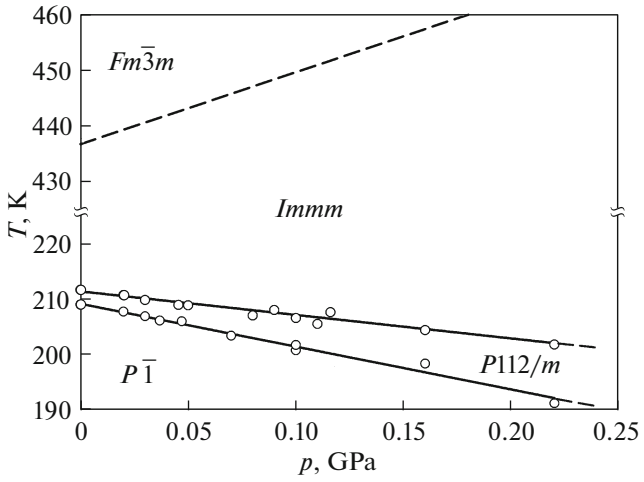

Fig. 4. Temperature–pressure phase diagram of the $(ND_4)_3VO_2F_4$ crystal. The interface line between phases $Fm\bar{3}m$ and $Immm$ (the dashed line) was recovered based on calculation of $(dT_1/dp)_{calc}$.

The temperature dependence of tanδ is also characterized by a complex anomalous behavior at temperatures lower and higher than T_3 and T_4 that demonstrates an increase in the dielectric losses (Fig. 5b). This is the reason why reliable measurements near the phase transition at T_1 were hampered. Dependences $\varepsilon(T)$ and tan $\delta(T)$ demonstrate significant hysteric phenomena in the region of the $Immm \leftrightarrow P112/m$ and $P112/m \leftrightarrow P\bar{1}$ phase transitions.

3. DISCUSSION OF THE RESULTS

The comparative analysis of the data obtained in the studies of $(ND_4)_3VO_2F_4$ in this work and $(NH_4)_3VO_2F_4$ in [19] enables us to make a number of conclusions with respect to the influence of deuteration on the phase transitions observed in the proton compound and, in particular, on the entropy and pressure parameters.

The high degree of deuteration (~87% D) did not influence the symmetry of the vanadium dioxotetrafluoride crystal at room temperature: it remained rhombic (space group *Immm*) in $(ND_4)_3VO_2F_4$. However, in this case, the unit cell volume substantially (~1.5%) increased as compared to that of the protonated vanadate [17]. It should be noted that the character and the degree of connection of the anion polyhedrons are likely to play a substantial role in the formation of size parameters of the crystal lattice. The D → H substitution in the $(NH_4)_2WO_2F_4$ and $(NH_4)_2MoO_2F_4$ oxyfluorides with isolated octahedrons led to a decrease in the unit cell volume by ~0.2% [25, 26].

We did not observe anomalies in the behavior of the thermodynamic properties of $(ND_4)_3VO_2F_4$ that could be related to the $Immm \leftrightarrow$ rhombic phase phase transition observed in $(NH_4)_3VO_2F_4$ at T_2 (Table 2) [18, 19]. That is, the change in the chemical pressure related to the increase in the unit cell volume led to the realization of the direct $Immm \leftrightarrow P112/m$ phase transition in $(ND_4)_3VO_2F_4$.

The integration of the temperature dependences of the anomalous heat capacities (Figs. 2a and 6a) enabled us to state the values and the behavior of the entropy related to the sequence of the phase transitions $\Delta S_i(T) = \int(\Delta C_p/T)dT$ (Fig. 2b). Because the

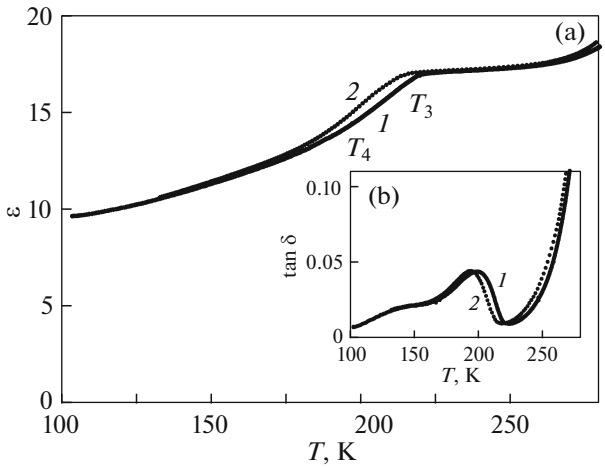

Fig. 5. Temperature dependences of (a) permittivity $\varepsilon(T)$ and (b) dielectric losses $\tan\delta(T)$ measured on (*1*) heating and (*2*) cooling.

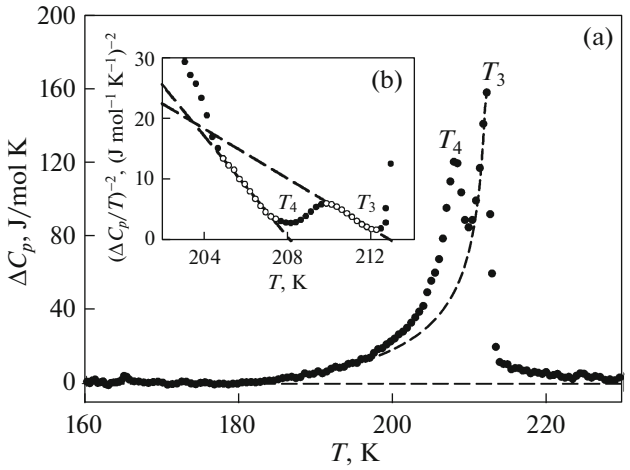

Fig. 6. Temperature dependences of (a) the excess heat capacity and (b) the squares of its reverse value near T_3 and T_4.

$Fm\bar{3}m \leftrightarrow Immm$ structural transformation was far from the low-temperature phase transitions (Fig. 2a), it was easy to determine the entropy change at T_1 (Table 2). For the $Immm \leftrightarrow P112/m$ and $P112/m \leftrightarrow P\bar{1}$ phase transitions that take place at very close temperatures T_3 and T_4, only the summary entropy change $\Delta S_3 + \Delta S_4 = 5.8 \pm 0.5$ J/(mol K) was determined at the first stage. To determine the individual entropies, we used the approach that we successfully used to separate the anomalous heat capacities in phases $P112/m$ and $P\bar{1}$ of oxyfluoride $(NH_4)_3VO_2F_4$ [19].

The existence of the excess heat capacity in quite wide temperature ranges below T_3 and T_4 (Fig. 6a) makes it possible to analyze its behavior in the framework of the Landau thermodynamic theory. According to one of the consequences of this theory [28], the square of the reciprocal excess heat capacity is a linear function of temperature $(\Delta C_p/T)^{-2} = [2(B^2 - 3A'C)^{0.5}/A_T^2]^2 + 12C(T_0 - T)/A_T^3$. Here, the quantities $A_T(T_0 - T_C) + A_T(T - T_0) = A' + A_T(T - T_0) = A$, B, and C are the coefficients of the thermodynamic potential: $\Delta\Phi(p, T, \eta) = A\eta^2 + B\eta^4 + C\eta^6$ (η is the parameter of the transition, T_C is the Curie temperature, and T_0 is the phase transition temperature).

The data presented in Fig. 6b show that, at temperatures lower than T_3 and T_4, the temperature behavior of the square of the reverse excess heat capacity of $(ND_4)_3VO_2F_4$ is actually described by linear temperature dependences. This allowed us to separate the individual contributions of the anomalous heat capacities by the extrapolation of the $(\Delta C_p/T)^{-2}(T)$ related to the $Immm \leftrightarrow P112/m$ phase transformation on the temperature range lower than T_4 (Fig. 6a) and, thus, to find the individual phase transition entropies ΔS_3 and ΔS_4 (Table 2).

We used the $(\Delta C_p/T)^{-2}(T)$ dependences to determine the relationships between the coefficients of thermodynamic potential A_T^2/B and A_T^3/C that were used to estimate dimensional T_i and T_{Ci} and dimensionless $N_i = \pm[B^2/(3A_TCT_{Ci})]^{-0.5}$ parameters that characterize the proximity of the phase transitions to the tricritical point (Table 2). The stepwise changes in the entropy (Fig. 2b) and deformation (Fig. 3a) during phase transitions show that $(ND_4)_3VO_2F_4$ undergoes the first-order transformation. According to these results, the calculated values of N_i for the $Immm \leftrightarrow P112/m$ and $P112/m \leftrightarrow P\bar{1}$ phase transitions have the negative sign (Table 2). From the comparison of the dimensional and dimensionless parameters, it follows that the transition at T_4 in $(ND_4)_3VO_2F_4$ is substantially closer to the tricritical point that is characterized conditions $T_i - T_{Ci} = 0$ and $N = 0$. On the one hand, the deuteration insignificantly influenced the parameters $T_3 - T_{C3}$ and N_3, on other hand, led to approaching the transition at T_4 to the tricritical point.

As abovementioned, it was impossible, because of technical problems, to experimentally studied the pressure susceptibility of the $(ND_4)_3VO_2F_4$ in the region of the high-temperature $Fm\bar{3}m \leftrightarrow Immm$ phase transition. However, the existence of the data on the entropy jumps $\delta S_1 \approx 4.8$ J/(mol K) (Fig. 2b) and deformation jump $\delta(\Delta V/V_0)_{T1} = 0.006$ (Fig. 3a) enables the calculation of the corresponding pressure coefficient $(dT_1/dp)_{calc}$ (Table 2), using the Clapeyron–Clausius.

Pressure coefficients dT_i/dp for the low-temperature phase transitions that take place in the $(ND_4)_3VO_2F_4$ crystal at T_3 and T_4 were determined using two methods: first, the direct measurements of the shift in the temperature under pressure $(dT_i/dp)_{exp}$ and, second, the calculation of $(dT_i/dp)_{calc}$ in the terms of the Pippard relationship $C_p = \beta VT_i/(dT_i/dp)_{p=0}$ + const [29] (Table 2) using the experimental dependences $C_p(T)$ and $\beta(T)$. Taking into account that the problems appeared when determining correct temperature dependences β at temperatures lower than T_3 and T_4, we can consider the agreement between the experimental and calculated pressure coefficients satisfying, which also indicates the reliability of the results of the independent experiments.

In [19], the pressure coefficient for the $Fm\bar{3}m \leftrightarrow Immm$ phase transition in $(NH_4)_3VO_2F_4$ was not determined. However, according to the relation between the values of dT_3/dp and dT_4/dp in both vanadates, we can suppose to a high degree of reliability that, at least, $dT_1/dp > 0$ also takes place in $(NH_4)_3VO_2F_4$. Thus, significant expansion of the temperature range of exis-

tence of the rhombic *Immm* phase under pressure is characteristic of both oxyfluorides $(ND_4)_3VO_2F_4$ and $(NH_4)_3VO_2F_4$.

In the deuterated crystal, the rate of decrease in the temperatures of the difference between them $Immm \leftrightarrow P112/m$ and $P112/m \leftrightarrow P\bar{1}$ phase transitions substantially increases under pressure, and the difference between them increases (Table 2). It is quite probable that this can be related to the absence of the second rhombic phase in $(ND_4)_3VO_2F_4$. As a result, the stability of the monoclinic and triclinic phases is retained to lower temperatures with the increase in pressure; and the pressure leading to the suppression of phase $P\bar{1}$ for $(ND_4)_3VO_2F_4$ is significantly lower (~2.7 GPa) than that for $(NH_4)_3VO_2F_4$ (~8.2 GPa).

According to the data given in Table 2, the deuteration led to change in the temperatures of the $Fm\bar{3}m \leftrightarrow Immm$, $Immm \leftrightarrow P112/m$, and $P112/m \leftrightarrow P\bar{1}$ phase transitions as compared to the protonated crystal. In this case, the character of changes in the temperatures are different: T_1 decreases by ~1 K, and T_3 and T_4 increase by ~2 K and ~3 K, respectively. Such changes in the transition temperatures agree with the positive pressure coefficient of the $Fm\bar{3}m \leftrightarrow Immm$ transition (Table 2) and the temperature–pressure phase diagram including subsequent $Immm \leftrightarrow P112/m \leftrightarrow P\bar{1}$ in the $(NH_4)_3VO_2F_4$ crystal [19]. Actually, the abovementioned increase in the unit cell volume in the deuterated vanadate can be considered to be related to a decrease in the chemical pressure in the crystal lattice. The calculated absolute value of negative pressure ($\Delta p \approx -0.08$ GPa) for the $(ND_4)_3VO_2F_4$ crystal was substantially higher than the pressure ($\Delta p \approx 0.02$ GPa) that occurs upon deuteration of ammonium oxyfluoride with isolated $(ND_4)_2MoO_2F_4$ octahedrons [25, 26]. It is not inconceivable that significant value Δp can be the reason of the abovementioned absence of the anomaly of the physical properties of $(ND_4)_3VO_2F_4$ observed in the protonated crystal at $T_2 \approx 244$ K and related to the $Immm \leftrightarrow$ rhombic phase [19].

As a result of the complex twinning of the crystal, the polarization-optical study did not enable us to make unambiguous conclusion on the ferroelastic nature of the phase transitions in $(NH_4)_3VO_2F_4$ [18]. However, the choice of the centrosymmetric space groups allows us to believe that the physical nature of the structural transformations is not ferroelectric. The dielectric studies also supported this assumption: small anomalies in dependences $\varepsilon(T)$ [19] were interpreted according to [30] as anomalies related to the structural distortions that were not accompanied by the appearance of polar phases. In this work, we did not observed significant anomalies of the dielectric permittivity and the dielectric loss also for $(ND_4)_3VO_2F_4$. Thus, the nature of the phase transitions in complex oxyfluoride vanadates is not dependent on the tetrahedral polyhedron composition.

The deuteration led to some decrease in the individual entropies of the $Fm\bar{3}m \leftrightarrow Immm$ and $Immm \leftrightarrow P112/m$ phase transitions and did not cause changes in the entropy of the displacement-type $P112/m \leftrightarrow P\bar{1}$ transition (Table 2). As a result, we also observed the decrease in the summary entropy changes $\Sigma\Delta S_i$ related to the distortion of the structure as the crystal lattice symmetry is reduced from the cubic $Fm\bar{3}m$ to the triclinic $P\bar{1}$: $\Sigma\Delta S_i \approx 14.5 \pm 1.7$ J/(mol K) = $(1.74 \pm 0.20)R$ for $(ND_4)_3VO_2F_4$ and $\Sigma\Delta S_i \approx 16.9 \pm 1.9$ J/(mol K) = $(2.03 \pm 0.23)R$ for $(NH_4)_3VO_2F_4$ [19].

The $(NH_4)_3VO_2F_4$ compound is a remarkable exclusion among ammonium oxyfluorides, since for it, first, the crystal systems were determined for all phases [18] and, second, the structure of the first distorted *Immm* (*I*222) phase was refined [17, 20]. The symmetry of the cubic $Fm\bar{3}m$ phase for $(NH_4)_3VO_2F_4$ was chosen by analogy with the relative $(NH_4)_3VOF_5$ vanadate for which structure was refined at temperatures higher than T_1 [20]. When analyzing the structure, the preference was given to a model in which central V atom was displaced in the direction of an edge of the octahedron formed by two oxygen atoms, since this variant of disordering leads to a some decrease in the *R*-factor. In this case, all anion polyhedrons must have 12 space orientations in the $Fm\bar{3}m$ phase. The ammonium groups are also considered disordered, but to different degrees of disorder: the tetrahedrons in positions 8*c* (two thirds tetrahedrons) and 4*b* (one third tetrahedrons) have four and eight space orientations, respectively [20].

Within this structural model, the complete ordering of anion and cation polyhedrons must be accompanied by the entropy changes: $R\ln 12 + 2/3R\ln 4 + 1/3R\ln 8 = 34.1$ J/(mol K) = $R\ln 60$. This is significantly larger than the values found experimentally: $\Sigma\Delta S_i \approx R\ln 6$ for $(ND_4)_3VO_2F_4$ and $\Sigma\Delta S_i \approx R\ln 8$ for $(NH_4)_3VO_2F_4$.

It could be assumed that this difference is due to the existence of additional phase transitions at lower temperatures, as compared to those that were attained in the calorimetric experiments (~100 K). Actually, despite the triclinic symmetry of the phase below T_4, we can well assume the existence of a change in the structure with increase of the symmetry as temperature decreases, as it was observed, for example, in double fluoride salts with analogous initial $Fm\bar{3}m$ phase [31]. However, the studies of the Raman and IR spectra up to $T \approx 8$ K did not reveal any evidence in favor of the existence other phase transitions in addition to the known transitions [32].

It should be noted that the entropy changes in the vanadates under study in a good agreement with anal-

ogous parameters of relative ammonium compounds with the initial cubic $Fm\bar{3}m$ symmetry, but with other compositions and the symmetry of oxyfluoride octahedrons C_{4v} ($(NH_4)_3TiOF_5$) ($\Sigma\Delta S_i \approx 2.18R$) and C_{3v} ($(NH_4)_3WO_3F_3$) ($\Sigma\Delta S_i \approx 2.03R$) [33], for which the refinement of the distorted phase structures was not carried out because of the formation of a complex twin structure upon the phase transitions [34]. A comparison of these data with the date for cubic fluorides undergoing significant structural distortions as a result of sequential phase transitions: $Fm\bar{3}m \leftrightarrow P2_1/n \leftrightarrow I2/m \leftrightarrow I\bar{1}$ ($(NH_4)_3ScF_6$: $\Sigma\Delta S_i$ = 23 J/(mol K) = $2.77R$) or direct phase transition $Fm\bar{3}m \leftrightarrow I\bar{1}$ ($(NH_4)_3GaF_6$: $\Sigma\Delta S$ = 23 J/(mol K) = $2.77R$) [35] shows that the degree of disordering structural elements in complex fluorides is substantially higher. Thus, the symmetry of six-coordinated anion polyhedron that is higher in fluorides (O_h) than that in vanadium oxyfluorides (C_{2v}). Actually, the results of numerous experimental calorimetric studies showed that the maximum values of the phase transition entropy in ammonium oxyfluorides, in which the framework of the crystal lattice is formed by six-coordinated anion polyhedrons are not higher than $\Sigma\Delta S_i$ = 2.1 R and $\Sigma\Delta S_i$ = 2.8 R [23].

From our point of view, the giant changes in the entropy that follow from model concepts of disordering all structural elements in the $Fm\bar{3}m$ phase should be considered to be limitedly possible. And this circumstance is of undeniable interest from the point of view of possibility of developing high-efficient solid-state barocaloric coolants, for which high phase transition entropy is a very important parameter [36]; i.e., we should find the means of influence on the degree of disordering structural elements. Significant differences between the experimental and model phase transition entropies in complex oxyfluorides enable the assumption that, for some critical ions, significant anharmonism of vibrations is characteristic, rather than a disordering over several crystallographic positions. In this case, the entropy change is proportional to the anharmonicity parameter $\delta = \langle x \rangle^2/a^2$ that relates the ion vibration amplitude x with a mean interatomic distance a [37] and can be substantially smaller than that following from the order–disorder model. In this connection, attention should be drawn to the fact that the decrease in the entropy in $(ND_4)_3VO_2F_4$ as compared to that in $(NH_4)_3VO_2F_4$ (Table 2) took place only for the order–disorder phase transitions at T_1 and T_3. Entropy ΔS_4 for the displacement-type phase transition was changed only slightly. Thus, it is not inconceivable that the deuteration led to a decrease in the degree of anharmonicity of vibrations of tetrahedral cations.

4. CONCLUSIONS

The crystals of deuterated vanadium dioxotetrafluoride $(ND_4)_3VO_2F_4$ have been grown and their thermal physical properties have been studied in a wide temperature range.

It is found that the unit cell volume of $(ND_4)_3VO_2F_4$ is significantly higher than that of $(NH_4)_3VO_2F_4$ (~1.5%), which led to a change in the chemical pressure that causes a number of changes in the pattern of structural transformations having place in the protonated vanadate.

(1) The secondary rhombic phase in $(ND_4)_3VO_2F_4$ is wedged out and the direct $Immm \leftrightarrow P112/m$ transition takes place instead sequential phase transitions: $Immm \leftrightarrow$ rhombic phase $\leftrightarrow P112/m$.

(2) The comparison of dimensional T_0-T_C and dimensionless N parameters shows that the transition at T_4 is substantially close to the tricritical point and significantly approaches it as a result of the deuteration.

(3) The pressure coefficients have been determined and the temperature–pressure phase diagram has been built. From the diagram, it follows that the pressure increase is accompanied by the expansion of the temperature region of the stability of rhombic phase *Immm* and a faster suppression of the triclinic phase in $(ND_4)_3VO_2F_4$. The change in the phase transition temperatures as a result of the D $\rightarrow$ H substitution agrees with the decrease in the chemical pressure provided by the increase in the unit cell volume.

(4) The dielectric studies showed that the phase transition nature remains nonferroelectric, despite all the changes of physical properties as a result of the deuteration.

(5) The summary experimental entropies of the transitions at T_1 and T_3 in $(ND_4)_3VO_2F_4$ ($\Sigma\Delta S_i \approx R\ln 6$) and $(NH_4)_3VO_2F_4$ ($\Sigma\Delta S_i \approx R\ln 8$) are significantly smaller than the entropies that are obtained from the model of disordering of structural elements in the $Fm\bar{3}m$ phase ($\Sigma\Delta S_i \approx R\ln 60$) [20] which most likely can be considered to be maximum possible for oxyfluoride vanadates. The decrease in the total entropy $\Sigma\Delta S_i$ as a result of the deuteration demonstrates to a great fraction of the probability significant (but not limiting corresponding to disordering) anharmonism vibrations of ammonium tetrahedrons.

ACKNOWLEDGMENTS

The reported study was funded by Russian Foundation for Basic Research, Government of Krasnoyarsk Territory, Krasnoyarsk Regional Fund of Science to the research project: "Effect of deuterium on orientational ordering and phase transitions in ammonium fluorine oxygen vanadates," no. 18-42-243003.

REFERENCES

1. H.-Y. Chang, S.-H. Kim, P. S. Halasyamani, and K. M. Ok, J. Am. Chem. Soc. **131**, 2426 (2009).
2. E. C. Glor, S. M. Blau, J. Yeon, M. Zeller, P. Shiv Halasyamani, J. Schrier, and A. J. Norquist, J. Solid State Chem. **184**, 1445 (2011).
3. Y. Inaguma, M. Yoshida, and T. Katsumata, J. Am. Chem. Soc. **130**, 6704 (2008).
4. M. Marvel, J. Lesage, J. Baek, P. S. Halasyamani, C. L. Stern, and K. R. Poeppelmeier, J. Am. Chem. Soc. **129**, 13963 (2007).
5. R. Gautier, K. B. Chang, and K. R. Poeppelmeier, Inorg. Chem. **54** (4), 1712 (2015).
6. P. A. Maggard, A. L. Kopf, C. L. Stern, and K. R. Poeppelmeier, Cryst. Eng. Commun. **6**, 451 (2004).
7. P. Halasyamani, K. R. Heier, M. J. Willis, C. L. Stern, and K. R. Poeppelmeier, Z. Anorg. Allg. Chem. **622**, 479 (1996).
8. S. Halasyamani, K. R. Heier, C. L. Stern, and K. R. Poeppelmeier, Acta Crystallogr., C **53**, 1240 (1997).
9. P. A. Maggard, A. L. Kopf, C. L. Stern, K. R. Poeppelmeier, K. M. Ok, and P. S. Halasyamani, Inorg. Chem. **41**, 4852 (2002).
10. R. Gautier, M. D. Donakowski, and K. R. Poeppelmeier, J. Solid State Chem. **195**, 132 (2012).
11. D. W. Aldous and P. Lightfoot, Solid State Sci. **11**, 315 (2009).
12. R. A. F. Pinlac, C. L. Stern, and K. R. Poeppelmeier, Crystals **1**, 3 (2011).
13. R. Gautier, M. D. Donakowski, and K. R. Poeppelmeier, J. Solid State Chem. **195**, 132 (2012).
14. N. F. Stephens, M. Buck, and P. J. Lightfoot, J. Mater. Chem. **15**, 4298 (2005).
15. R. R. Ryan, S. H. Mastin, and M. J. Reisfeld, Acta Crystallogr., B **27**, 1270 (1971).
16. S. J. Patwe, A. S. Nagabhusan, K. G. Girija, C. G. Sivan Pillai, and A. K. Tyagi, J. Mater. Res. **25**, 1251 (2010).
17. M. Leimkühler and R. J. Mattes, Solid State Chem. **65**, 260 (1986).
18. S. V. Mel'nikova and A. G. Kocharova, Phys. Solid State **51**, 597 (2009).
19. V. D. Fokina, M. V. Gorev, A. G. Kocharova, E. I. Pogoreltsev, and I. N. Flerov, Solid State Sci. **11**, 836 (2009).
20. A. A. Udovenko, E. I. Pogoreltsev, Y. V. Marchenko, and N. M. Laptash, Acta Crystallogr., B **73**, 1 (2017).
21. R. L. Withers, F. J. Brink, Yu. Liu, and L. Noreın, Polyhedron **26**, 290 (2007).
22. A. A. Udovenko and N. M. Laptash, Acta Crystallogr. B **67**, 447 (2011).
23. I. N. Flerov, M. V. Gorev, M. S. Molokeev, and N. M. Laptash, in *Photonic and Electronic Properties of Fluoride Materials*, Progress in Fluorine Science Series, Ed. by A. Tressaud and K. Poeppelmeier (Elsevier, Amsterdam, 2016), p. 355.
24. E. V. Bogdanov, A. D. Vasil'ev, I. N. Flerov, and N. M. Laptash, Phys. Solid State **53**, 303 (2011).
25. I. N. Flerov, V. D. Fokina, M. V. Gorev, E. V. Bogdanov, M. S. Molokeev, A. F. Bovina, and A. G. Kocharova, Phys. Solid State **49**, 1149 (2007).
26. E. V. Bogdanov, E. I. Pogoreltsev, M. V. Gorev, and I. N. Flerov, Inorg. Chem. **56**, 6706 (2017).
27. *Bruker AXS TOPAS V4: General Profile and Structure Analysis Software for Powder Diffraction Data, User's Manual* (Bruker AXS, Karlsruhe, Germany, 2008).
28. K. S. Aleksandrov and I. N. Flerov, Sov. Phys. Solid State **21**, 195 (1979).
29. N. Parsonidzh and L. Steivli, *Disorder in Crystals* (Mir, Moscow, 1982).
30. B. A. Strukov and A. P. Levanyuk, *Physical Principles of Ferroelectric Phenomena* (Nauka, Moscow, 1983) [in Russian].
31. M. Molokeev, S. V. Misjul, I. N. Flerov, and N. M. Laptash, Acta Crystallogr. B **70**, 924 (2014).
32. Yu. V. Gerasimova, A. S. Oreshonkov, N. M. Laptash, A. N. Vtyurin, A. S. Krylov, N. P. Shestakov, A. A. Ershov, and A. G. Kocharova, Spectrochim. Acta A **176**, 106 (2017).
33. I. N. Flerov, M. V. Gorev, V. D. Fokina, A. F. Bovina, and N. M. Laptash, Phys. Solid State **46**, 915 (2004).
34. A. A. Udovenko and N. M. Laptash, Acta Crystallogr., B **67**, 447 (2011).
35. M. V. Gorev, I. N. Flerov, and A. Tressaud, J. Phys.: Condens. Matter **11**, 7493 (1999).
36. M. V. Gorev, E. V. Bogdanov, and I. N. Flerov, J. Phys. D **50**, 384002 (2017).
37. V. G. Vaks, *Introduction to the Microscopic Theory of Ferroelectrics* (Nauka, Moscow, 1973) [in Russian].

Translated by Yu. Ryzhkov